

Intelligent Technique for Grading Tropical Fruit using Magnetic Resonance Imaging

Wasiu A. Balogun, Momoh-Jimoh E. Salami, Michael J. McCarthy, Yasir M. Mustafah, Abiodun M. Aibinu

Abstract— Recent application of modern marketing techniques coupled with intelligent agricultural systems of production has transformed small scale farming into large scale, in most part of the world. Characteristically, most of the tropical fruits, such as orange, appeared edible physically but internally such fruits might be defective based on their tissue and juice. Eventually, these fruits, via the market and undetected, usually get to the consumers who encounter the unfavourable status of the fruits. Our purpose, in this study, is to develop a non-destructive method to predict the status of orange fruits, based on internal quality. Graph of histogram showing the levels of different four colour intensities were acquired and analysed. The features extracted from Magnetic Resonance Imaging (MRI), using any of the two proposed methods, were applied as an input to train artificial neural network (ANN) in order to predict the orange fruit status. Different structures of multi-layer perceptron neural networks with feed-forward and back-propagation learning algorithms were developed using MATLAB. The theoretical background of MRI and artificial neural network (ANN) backpropagation were also explained. At hidden neuron value of 20, search is for backpropagation and number of neurons in the hidden layer to optimize the ANN. Levenberg-Marquardt algorithm (trainlm) gave the best performance fitness out of different types of backpropagation algorithm used with least Mean Square Error (MSE) of 0.0814 corresponding to R-value of 0.8094. This work shows that ANN and MRI have the capability of predicting the internal content and detect defect fruit based on water proton content.

Index Terms: Magnetic Resonance Imaging, Artificial Neural Network, image analysis, internal quality, backpropagation algorithm.

1. INTRODUCTION

Traditionally, quality inspection techniques of fruits have been manual, but these have been highly inconsistent in accuracy, time consuming, tedious and relatively expensive. Thus, the application of new techniques in fruit quality assessment is necessary in order to minimise wastage because most of these fruits are readily perishable. Furthermore, fruit quality grading is becoming a mandatory condition in recent time, although quality of fresh fruits could be defined differently depending on a consumer's preference and final utility, but a standardization to identify the degree of quality in a commodity is necessary for marketing fresh and safe products. Common varieties of tropical fruits sold and consumed widely include oranges, watermelon, grapes, bananas, avocado, papaya and pineapples.

Grading of fruit is essentially based on external quality assessment which is commonly applied and internal quality

grading which is seldom used (Du and Sun, [1]). Major fruit's quality factors includes size, shape, colour, defects (external quality) and nutrition, defect, texture, flavour (internal quality) (Du and Sun [1], Barreiro et al [2], Ruiz-Altisent et al [3], Kleyne et al [4]).

The introduction of different techniques to determine the internal quality of fruits is becoming a principal challenge in recent time. Most of the techniques currently used for internal quality measurement operate in a destructive mode, however, non-destructive quality evaluations of fruit product is becoming necessary for agricultural and food industry (Du and Sun, [1]).

Various non-destructive methods, such as ultrasonic, vibrated excitation, impedance, laser spectroscopy, reflectance, X-ray Imaging, transmittance, absorbance spectroscopy and near infrared imaging (NIR) have been developed to assess the internal fruit quality (Yacob et al [5]). Meanwhile, their industrial applications to fruit quality grading remains limited due to problems with accuracy and methodology. On the other hand MRI allows a non-destructive study of the internal properties of fruits and applying this at a low time cost would bring a desirable added value to the product (Ruiz-Altisent et al [3], Zion et al [6], Kerr et al [7]).

The Image processing method facilitates automatic fruit grading via precise, consistent, reliable and quantitative information, particularly, when handling large volume of fruits. Tropical fruits that are internally defective hardly show any sign of damages on their rinds, thus making those fruits unfit for eating or used for industrial purposes (Ruiz-Altisent et al [3], Yacob et al [5]).

- *Corresponding Author: Balogun Wasiu Adebayo, MIEEE, currently pursuing a postgraduate degree program in Mechatronics Engineering in International Islamic University (IIUM), 53100, Gombak, Malaysia. A Research Scholar, University of California, Davis, United State of America. E-mail:balogunwa1999@yahoo.com*
- *Co-Author 1: Momoh-Jimoh E. Salami is a Professor in the Department of Mechatronics Engineering, IIUM, Malaysia. E-mail:momoh@iium.edu.my*
- *Co-Author 2: Michael J. McCarthy is a Department Chair and a Professor in the Department of Food Science and Technology, University of California, Davis, United State of America. Email:mjmcCarthy@ucdavis.edu*
- *Co-Author 3: Yasir M. Mustafah is an Asst. Professor in the Dept. of Mechatronics Engineering, IIUM, Malaysia. E-mail:yasir@iium.edu.my*
- *Co-Author 4: Abiodun M. Aibinu, was with International Islamic University Malaysia. He is now with Electrical Engineering Dept., Federal University of Technology, Minna, Niger State Nigeria. E-mail: maibinu@gmail.com.*

MRI is an imaging technique that utilized the magnetic properties of nuclei in relation with radio frequency and magnetic field. It is sensitive to the local environment of water and oil which are main composition of fruit. Furthermore, MRI is used to acquire two as well as three-dimensional images of biological systems from obscured materials. It predict the tomato maturity with PLS-DA model for classification and shows that different maturity stages are embedded in MR images signal intensity (Zhang and McCarthy[8]).

The viability of MRI to distinguish frozen-thawed products such as Kiwis (Kerr et al [7]) blueberries (Gamble [9]), and courgettes (Duce et al [10]) by means of changes in the contrast of the magnetic resonance images have been studied. A recent study have shown a longitudinal NMR parameter measurement of Japanese pear fruit during the growing process using a mobile magnetic resonance imaging system to determine the relaxation times and diffusion coefficients of the fruit relative to the weight. This justified the reliability of MRI for determining the internal quality of the outdoor pear (Geya et al [11]).

The usage of MRI in detecting freeze damage in fruit was reported. An algorithm was applied to extract several mathematical features for the characterization of each sample and the fruits were cut for visual inspection and performed reference classification, after preliminary analysis, (Barreiro et al [2]).

Milczarek et al in [12] developed a method to determine injured pericarp tissue in tomatoes using MRI equipment. Samples of heavily bruised and non-bruised tomatoes were manually selected on a conveyor and each was inserted into the bore of an industrial-grade (1T) MR imaging system Aspect AI, with the stem/calyx axis along the (horizontal) bore. Thirteen MR images were obtained for each sample, while the Fast Spin Echo (FSE) image had an effective echo time of 281 ms and produces T2-weighted contrast in the images. After imaging, the samples pericarp were analysed in the conductivity test. The hyper-intense pericarp pixels indicate areas of high conductivity result for extensively bad membrane and hypo-intense pericarp pixels for good membrane.

MRI has been used to measure the moisture and oil content of agricultural materials showing a difference between image pixels corresponding to good and damage tissue. The internal damage resulting from core breakdown and browning can be easily detected in pears and apples fruit. This has also proved to be a reliable method to evaluate other fruit qualities such as ripening, core breakdown, bruises, worm, chilling and freezing damage. Thus, MRI methods have versatile application for fruits sorting and grading technology (Gonzalez et al [13], Hernandez-Sanchez et al [14]).

Efficient combination of colour and texture features for fruit recognition has been carried out by the minimum distance classifier based on the statistical and co-occurrence features derived from the Wavelet transformed sub-bands. This method is commonly applied as a class of techniques for segment-

ing out region of interest in an image. Background subtraction is derived from the subtraction of the observed image from the estimated image and thresholding the result to generate the images of interest. Finally, training and classification were applied using Minimum Distance Classifier (Arivazhagan et al [15]).

Yacob et al in [16] detected Harum Manis Mango weevil defect with the aid of dielectric sensor trained with neural network backpropagation. The procedure was repeated for data acquisition collected from thirty samples out of which sixteen samples for training and fourteen samples for testing. The training and testing started from upper epochs to lower epochs. They reported that B training set has higher rate of performance than set A with a learning rate of 0.01 and that smallest test error comes from set B which is 0.0870.

Automatic fruits identification systems with the combination of Fourier descriptors, artificial neural network and spatial domain analysis were proposed. The colour and shape information obtained from digital camera images of fruit samples were used as input to ANN training for fruit sorting and identification purpose by Aibinu et al in [17]. The application of neural network model to predict the vase life of cut roses planted in a greenhouse has shown that the ANN is better in prediction than traditional statistical techniques (In et al [18]).

The objectives of this study are to identify the ability of images obtained from MRI equipment in order to determine the internal quality of orange fruit sample based on defect (internally dry juice). Furthermore, an artificial neural network model using colour features of internally dry juice and good fruit derived from MRI images is to be developed for predicting the internal quality of the orange fruit.

2. MATERIAL AND METHODS

This section presents the methodology and development of algorithm for the implementation of the proposed intelligent fruit grading system (IFGS).

2.1. Samples

Orange samples used for this research were obtained from fruit market and were sorted, manually, into good (internal non-dry juice) and defect (internal dry juice) orange fruits by cutting for visual inspection.

2.2 Equipment

The MRI image data acquisition was performed using Aspect MRI equipment (Figure 1) at Professor, Michael J. McCarthy Laboratory, University of California, Davis, USA. The MRI system usually consists of hardware parts such as Electronics cabinet, Magnetic field gradient system, Permanent magnet, Radio-frequency system and Computer/Reconstruction system.

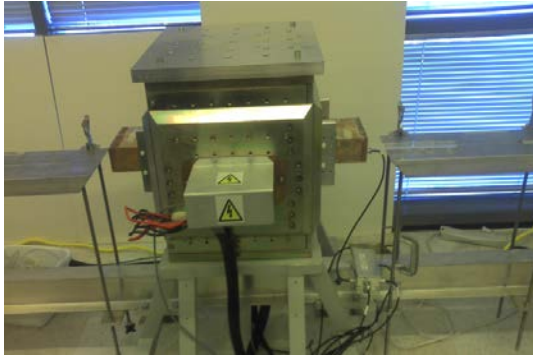


Figure 1: Aspect M2 MRI System

2.2.1 Basic MRI Theory

Spin: it is a fundamental part of nature like electrical charge which is in multiples of half ($1/2$) and can be positive or negative. Protons, electrons, and neutrons possess spin (Nishimura [19], Hashemi et al [20]).

Spin density: it is the density of mobile proton or the number of protons that possess enough mobility that can allow it to change direction and line up with the external magnetic field (Hashemi et al [20]).

Larmor Frequency: is the precessional frequency when nuclear spin exhibit resonance (Hashemi et al [20]).

T_1 recovery: (also known as longitudinal or Spin lattice relaxation time), is the recovery of magnetization along the axis of the external magnetic field B_0 . It is the period required for the Type equation here 63% of the longitudinal magnetisation to recover in the tissue (Nishimura [19]).

T_2 Decay: This is time constant characterizes the rate at which the M_{xy} component decays. It is caused by nuclei exchanging energy and defined as the period it takes 63% of the transverse magnetisation to be lost which is also known as spin-spin relaxation time (Nishimura [19]).

Free Induction Decay Signal (FID): This is the minimal voltage or signal 'S(t)' that is detected in the receiver coil due to the oscillating transverse component of the magnetisation after applying an RF pulse (Nishimura [19], Hashemi et al [20], Aibinu et al [21]).

RF Coils: it produces the magnetic field B_1 which rotates the net magnetization in a pulse sequence. It also detects the transverse magnetization as it is precise in the XY plane. There are three types: transmit and receive coils, receive coils and transmit coils only (Nishimura [19], Hashemi et al [20]).

Resonance: This occurs when the radio frequency pulse equals the frequency of precession of the protons.

Fast Fourier Transform (FFT): Conventionally, MRI is a Fourier transforms based method. Frequency or phase encoding is always carried out and the data obtained are kept in a line K-space, during data acquisition. Fast Fourier Transform technique is applied to convert the collected data in K-space to an image which is done by converting signal intensity in time domain to signal intensity in frequency domain, mathematically. It is also known as inverse Fourier transform (Nishimura [19], Aibinu et al [21], Aibinu et al [22]).

2.2.2 Basic MRI Equation

The Larmor equation (also known as Spin resonance equation) indicates the rate at which proton precesses around the external magnetic field (Hashemi et al [20]) stated in (1).

$$\omega = \gamma B_0 \tag{1}$$

Bloch Equation is the description of magnetisation dynamics. The Bloch equation is stated in (2).

$$\frac{dM}{dt} = M \times \gamma B - \frac{M_x i - M_y j}{T_2} + [\frac{M_z}{T_1} - \frac{M_z}{T_2}]k \tag{2}$$

The MRI equation is shown as follows in a 2D form as:

$$S(Kx, Ky) = f[(x, y)] \tag{3}$$

f stands for spatial information with inverse transform gives a data I as stated in (4).

$$I(x, y) = f^{-1} S(kx, Ky) \tag{4}$$

Image intensity $I(x, y)$ depends on $T_1 T_2 T_2^*$, ρ and D , which are Relaxation times, Spin density and Diffusion coefficients respectively (Zhang and McCarthy [8], Nishimura [19], Aibinu et al [21]) as stated in (5).

$$I = f[T_1, T_2, T_2^*, \rho, D] \tag{5}$$

With spin echo images, the intensity of the signal (S) of each pixel in the image is a function of intrinsic properties namely: Proton longitudinal (T_1), Proton density (PD), Transverse relaxation times (T_2) with the experimental values as the echo time (TE) and the repetition time (TR). The signal intensity (S) is stated in (6) (Zhang and McCarthy [8], Hashemi et al [20], Aibinu et al [21]).

$$S = K^* PD [1 - \exp(-T_R/T_1)] \exp(-T_E/T_2) \tag{6}$$

The model used for this work are broadly divided into the following stages applying two methods as shown in Figure 2 and the algorithms were developed with MATLAB.

2.3 Methods

The experiments were performed on a 1T permanent magnet Aspect MRI system (Figure 1) using a 60 x 90 cm elliptical RF

coil. The orange samples images were placed on a plastic sample holder and position manually at the center such that the axis of the sample aligned with the center of the coil. During the alignment and de-alignment an emission and absorption of energy occurred in the RF of the electromagnetic. An image of the longitude slice was obtained along the axis of each sample orange with different sequences. Each sequence used was positioned such that all information on water proton is included in the MR image intensity and the pixels of each image were 128 x 128. Sixty-four MRI images slides were acquired from each fruit samples following steps described in table 1.

Table 1: Description of each step in the acquisition process (Aspect imaging [23]).

STEPS	DESCRIPTION
Set Sample	Open a record for the subject
Set Anatomy	Define how the subject is positioned in the device
Perform Scout	Perform a preliminary scan
Set Protocol	Select the protocol containing the scan sequences you require
Set Sequence	Select the scan sequence and modify the scan parameters if needed
Add to Queue	Add the sequence with the final parameters to the queue and run the sequence
Close Study	To start a new session with a new subject, close the session for the existing subject

2.4 PREPROCESSING

Feature extraction of Fruit: This is converting input data into a reduced representation set of features once the input data to an algorithm is too large for processing.

Histogram Intensity: Histogram is a graphical representation of data distribution used to enhance the image contrast or to determine the threshold values. This is a graph indicating the amount of pixels available in an image at each different intensity value located within the image. It gives compact information of data distribution in an image. It is the most used and easy way of representing colour in image processing which is known as histogram of the pixel intensity values.

In an 8-bit image gray scale there are 256 intensities and individual histogram of blue, red and green channels can be taken or a 3-D histogram with the three axes indicating blue, red and green channels, each point brightness indicating the pixel count. If there are only two objects in the image, histogram is always applied. (Fisher et al [24], Liang and Lauterbur [25], Gonzalez et al [26]).

If the intensity gray-level histogram is proportional to a function $z(g)$ with an intensity value each $g \in [0.....L]$ the quantity of pixels in the region of interest that have intensity equal to g is stated in equation 8 where N_g is the quantity of pixels in the region of interest or image that have intensity equal to g .

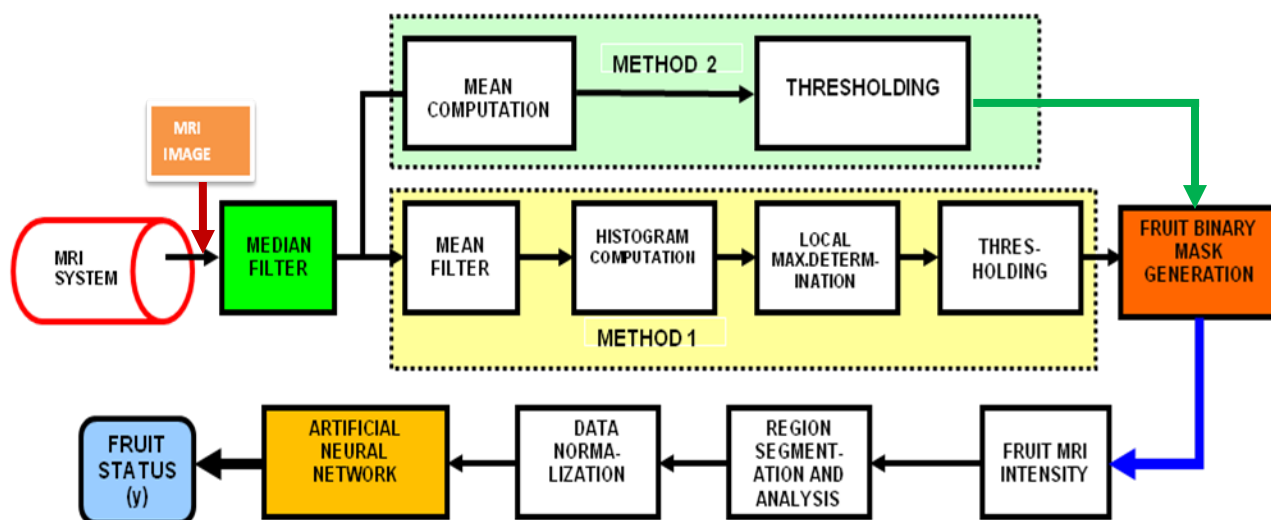


FIGURE 2: PROPOSED MODEL OF INTELLIGENT FRUIT GRADING SYSTEM

$$z(g) = N_g \tag{7}$$

Equation (7) leads to a function known as the probability density derived from normalization of histogram with the number of pixels in the image given in (8) as

$$p(g) = \frac{z(g)}{M} \tag{8}$$

The histogram is useful for thresholding since the information in the graph represent the pixel distribution as function of tonal variation. The obtained thresholding value can further be utilized for image segmentation, edge detection and co-occurrence matrices (Gonzalez et al [26], Bhaiya and Verma [27], Hecht-Nielsen [28]).

Image Segmentation: Involves splitting of images into respective regions and boundaries. If the right segmentation is used, it results to a strong level of interpretation of an image. This is a known method of dividing image intensity derived from the RGB components image into two non-overlapping, connected groups of pixels. There are four types of segmentation methods such as region, histogram, edge and classification segmentation (Du and Sun [1], Fisher et al [24], Gonzalez et al [26]).

Image Enhancement: MRI image consists of a high intensity salt and pepper noise present due to the gray scale variations in the image which is removed with the aid of suitable filters and performing normalization. Image enhancement techniques that remove noise without reducing the quality of the image normally uses mean, median, weighted median, Gabor, Gaussian and Adaptive filter (Gonzalez et al [26], Jayabalan [29]).

Descriptors: Images are normally presented in terms of two format namely external and internal characteristics. There are three types of descriptors that are used to indicate the pixel distribution and region based in image namely: Region descriptor, Boundary descriptors and Relational descriptors. Out of these, Region descriptor is used to quantify the texture content of an image in terms of coarseness, smoothness and regularity. However, the three main method for texture description of a region are Statistical, Structural and spectral (Gonzalez et al [26]).

Statistical Method: It is describe as the approach that uses the gray-level histogram to describe the properties of texture whether coarse, grainy, dry, wrinkled, rough, hard, soft, or smooth. Let Z , L and $P(z_i)$ stand for random variables indicating gray-level histogram, number of evident gray levels of intensity and corresponding histogram respectively. Then, the following are obtained. Mean (m) which is the average intensity is computed as

$$m = \sum_{i=0}^{L-1} (Z_i) p(Z_i) \tag{9}$$

Measure of Smoothness

$$R = 1 - \frac{1}{1 + \sigma^2} \tag{10}$$

Measure of Skewness of the histogram

$$\mu_3(z) = \sum_{i=0}^{L-1} (Z_i - m)^3 p(z_i) \tag{11}$$

Measure of Uniformity show another texture content as

$$U = \sum_{i=0}^{L-1} p^2(z_i) \tag{12}$$

Entropy is the measurement of randomness or variability of the image

$$e = - \sum_{i=0}^{L-1} p(z_i) \log_2 p(z_i) \tag{13}$$

Data Normalization: The features that will finally serves as input and output to neural network system should be in the same range in order to achieve high performance which is performed by normalization. The input and output features are normalized by (14) so that the mean is zero and the standard deviation is one.

$$f'_k = \frac{f_k - \mu(f_k)}{\sigma(f_k)} \tag{14}$$

Where f_k =initial values, f'_k =final values of a feature and $\mu(f_k)$ =mean, $\sigma(f_k)$ =standard deviation of class values belong to the image features. Finally, principal component analysis is then used on all the image features data set to avoid any variation (Gonzalez et al [26], Bhaiya and Verma [27], Hecht-Nielsen [28], Jayabalan [29]).

2.5 Artificial Neural Network Structure

Artificial Neural Network (ANN) was first introduced in 1943 by physiologists, McCulloch and Pitts as an interconnection of neurons that perform a process to produce an output. Its performance resemble that of human brain and when supply with enough samples, they can predict various variables such as daily temperature, climate and earthquake, detect or classify the presence of pests in vegetables and fruits, detect fault in assembly plant and even recognize human face and handwritten characters (Bhiya and Verma [27], Hecht-Nielsen [28], Kumar [30]).

The purpose of ANN is to generate a network system with little errors but also yield good result from the testing data set. There are two types of training algorithm namely: Supervised- the target is available and the network determines the best set of weights by reducing the error between the output data and

the target. Unsupervised - only the input data set is given to the system, which then determines similar inputs without any previous knowledge. (Hecht-Nielsen [28], Kumar [30]).

$$W_{ik}^{(j+1)} = W_{ik}^j - \eta \frac{\partial E^{(j)}}{\partial W_{ik}} \tag{17}$$

For this research work, prediction is achieved with the artificial neural network MATLAB. The study of techniques of prediction and diagnosis shows that the most widely used ANN is the three layers which comprises of input, hidden and output layer (Figure 3). The output result relies on the weight used on the data linking the output and hidden layers. During training and learning, weights are the value which ANN works on to realise a result that is very close to the required output. There should be a constant adjustment in the weight value equal to the error between output of network and the

Backpropagation Techniques: This is the most commonly used ANN architecture out of the entire neural network being applied to real world problems because it can easily learn complex multidimensional mappings. It is the process by which an artificial neural network adjusts the weights assigned to the connections between neurons to bring the current output data of the neuron closer to the expected data value (Hecht-Nielsen [28], Kumar [30]).

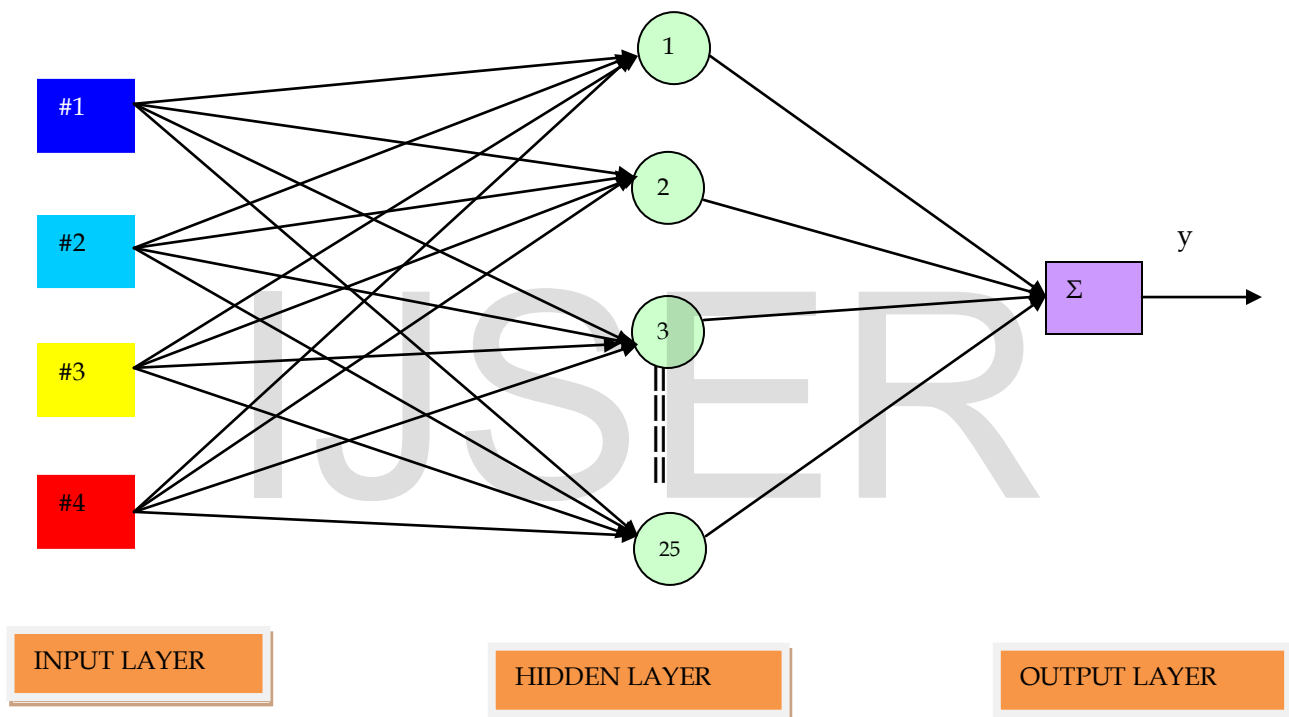


Figure 3: ANN Architecture for Fruit grading

actual output (Bhaiya and Verma [27], Hecht-Nielsen [28], Kumar [30]). The input layer linear neurons and hidden sigmoidal neuron equation is stated in (15) and (16) respectively.

$$\delta(x) = x \tag{15}$$

$$\delta(x) = \frac{1}{1 + e^{-\lambda x}} \tag{16}$$

Computation of input-to-hidden neurons is achieved with (17).

Backpropagation Terms

Epoch: An epoch is one presentation of the complete training set to the neural network.

Error: It is the differences between an expected neuron output value and the actual output value.

Hidden layer: Is a layer whose inputs and outputs value are connected to other neurons.

Neuron: It takes one or more input data value and changes them using an activation function to produce an output data.

Input layer: This is made up of neurons whose inputs are data that the network is expected to process.

Output layer: An output layer is a layer made up of neurons which output the end result of the network processing.

Overfitting: This occurs when the neural network begins to approximate individual data samples in the training set rather than generalizing the pattern that these data represented

shown in Figure 3. The input dimension is four colour intensity features, therefore the number of nodes in input layer is four and the number of nodes in output layer is one

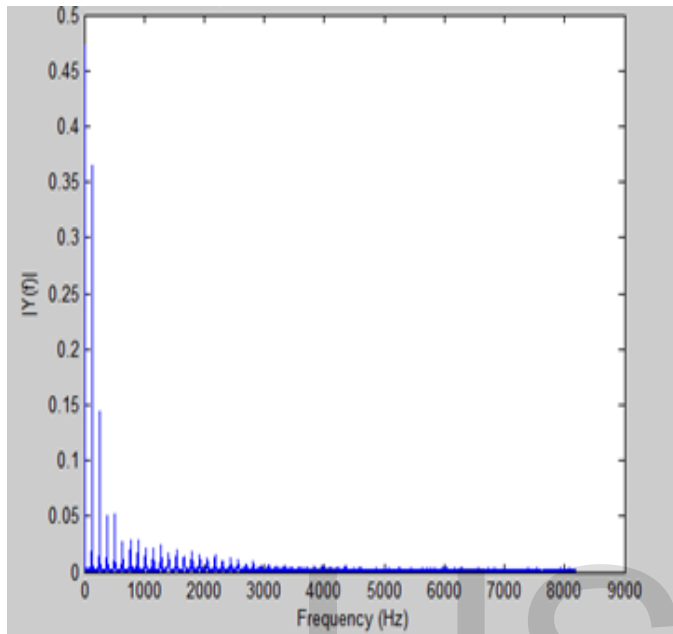


Figure 4: Histogram of defect orange image

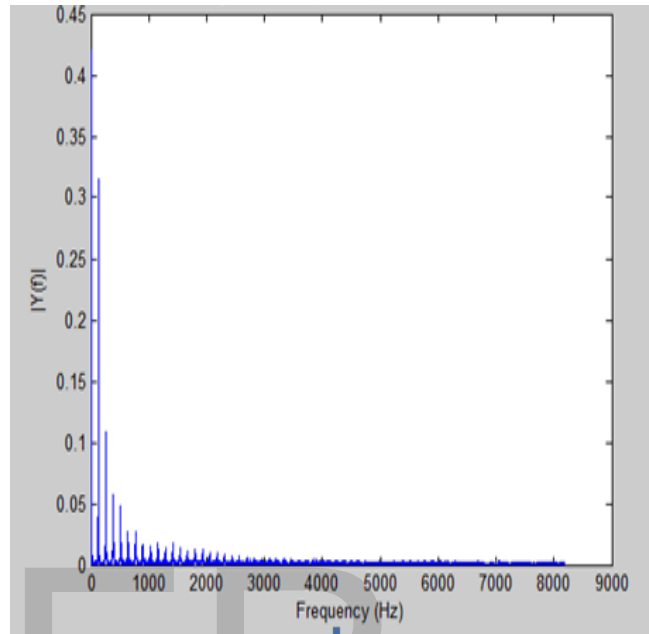


Figure 5: Histogram of good orange image

Mean square error (MSE): This is the mean of the squared differences between the expected and actual output data from neurons in a neural network. It is derived from a specific network over entire training set, stated in (18) with Q and ϵ_k stand for a set of training vector and instantaneous summed squared error respectively. (Bhiya and Verma [27], Hecht-Nielsen [28], Kumar [30]).

$$\epsilon = \frac{1}{Q} \sum_{k=1}^Q \epsilon_k \tag{18}$$

Training set: It is a set of samples that are used to train the network. Each sample in the training set includes the expected output data of the ANN

Symmetric sigmoid: is a type of activation function that is smooth and non-linear ranging from -1 to 1 (Bhiya and Verma [27], Hecht-Nielsen [28], Kumar [30]).

The orange images acquired from MRI were successfully reconstructed and processed to produce signal intensity data based on number of pixel obtained from region of interest (ROI) that served as an input to the neural network. The backpropagation proposed in this paper is three-tier model as

Table 2: Data set for the artificial neural network

Value of Data set	Normalized Parameters	Un-normalized Parameters
110	pn	Training Input p
110	tn	Training Output t
60	an	Testing Input a
60	sn	Testing Output s

The image features data (table 2) is divided into 110 training data sets for the input and output value and 60 data sets for testing value. These data sets were loaded into MATLAB workspace. The input and output layer neurons are linear purelin but the hidden layers are sigmoid signal function tan-sig.

3. RESULTS AND DISCUSSION

MRI images acquired were successfully processed with MATLAB code developed. Figure 4 and 5 shows one example

each of good and defect orange signal intensity histograms obtained from the segmented region of interest (ROI) of the image. There was a change in image texture explained with the histogram analysis. At the signal intensity value of the histogram the number of pixel is higher in defect orange getting to peak at 0.37 in Figure 4 compared with the histogram of good orange having a peak value of 0.32 as shown in Figure 5. These intensity features obtained from the MRI images serves as the input to the network.

In this study, important factors for using neural network is for internal quality prediction of the orange fruit depend on the proper selection of the following two parameters, namely fastest backpropagation and number of hidden neuron and the Corresponding value of mean square error and R-value. The neural network model considered in this work is three-tier model as shown in Figure 3. The dimension of the input vector and node used is four with one output node, twenty five hidden neuron numbers and fifty epochs.

Table 3: Backpropagation Algorithm used for training and Corresponding Correlation value

ALGORITHM	MSE VALUE	R VALUE
Resilient Backpropagation (trainrp)	0.1021	0.8346
Flecher-Reeves Conjugate Gradient (traincgf)	0.1098	0.7982
Polak-Ribiere Conjugate Gradient (traincgp)	0.0832	0.8654
Powell-Beale Conjugate Gradient (traincgb)	0.1164	0.7708
Levenberg-Marquardt (trainlm)	0.0814	0.8094
Scaled Conjugate Gradient (trainscg)	0.0959	0.8008
One Step Secant (trainoss)	0.1123	0.7454
BFGS Quasi-Newton (trainbfg)	0.1113	0.8211

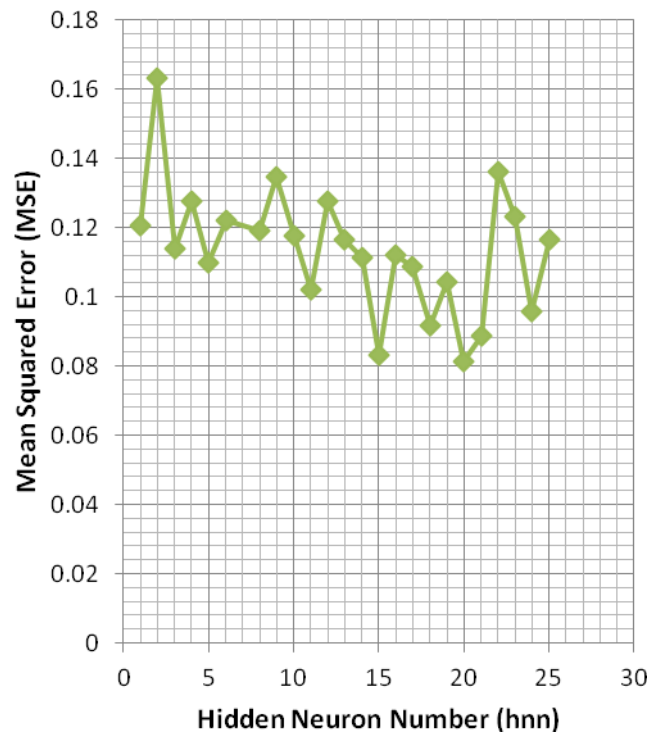


Figure 6: Plot of Hidden neuron number against Mean squared error

The images were randomly divided into three sets, one hundred and ten for training, sixty images for testing and validation. The output value is $y \in [1.0]$. If y is 1, it indicates that there is high possibility of good orange fruit (internal non-dry juice) and whereas if it is 0, it means that there is high possibility of defect orange fruit (internal dry juice). The list of eight used backpropagation algorithm considered in the study is shown in Table 3.

Optimization procedure of neural network architecture relies on adequate selection of neurons number in hidden layer that gives the lowest means squared error. Table 3, indicates eight used backpropagation algorithm and corresponding mean squared error (MSE) with regression value obtained. The ANN output and corresponding targets are in the post-processing regression analysis which feedback different values R-values.

The minimum mean squared error (MSE) obtained is 0.0814 which occurred at the optimum hidden neural number value of 20 as indicated in Figure 6. From Figure 7 and Table 3 the optimum preferable training algorithm is Levenberg-Marquadt (**trainlm**) backpropagation with R-value of 0.8094 which corresponds to the least mean squared error value.

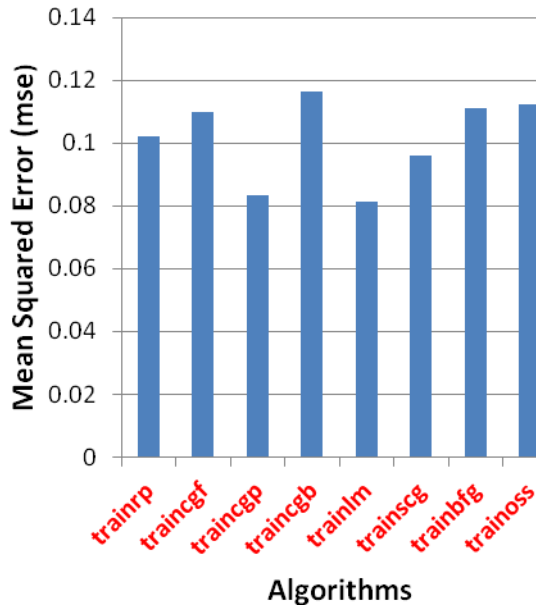


Figure 7: Plot of Training function algorithms with the corresponding Mean squared Error.

4. CONCLUSION

This study introduced the neural network method and tested its usefulness as an approach to classify MRI image of orange fruit into defect or good classes based on pixel intensity level. Therefore, imaging using MRI allow a high chance of determining internal quality of the fruit with a proper ANN model for prediction. Evaluation of models performance was tested based on R-value and mean squared error stated in Table 3.

The network with structure Levenberg-Marquardt (trainlm) algorithm backpropagation and twenty hidden neuron predicted the internal quality with maximum correlation coefficient R-value of 0.8094 coupled with the lowest mean squared error (MSE).

The result also showed that using different forms of training algorithm, high prediction accuracy can be achieved. The future work require development of more robust system with other neural network structural parameters and more image data so as to improve the model accuracy, since the higher the amount of input data, the lower the mean squared error.

ACKNOWLEDGMENT

The authors wish to thank Asst. Prof. Mecit Oztop and Dr Lu Zhang UC Davis, US, for their valuable guidance at every step in making this research work Successful.

REFERENCES

[1] C. J. Du, and Sun, D. W, "Recent developments in the applications of image processing techniques for food quality evaluation," *Trends in Food Science & Technology*, vol. 15, no. 5, pp. 230-

249, 2004.

[2] P. Barreiro, C. Zheng, D. Sun, N. Hernández-Sánchez, J. M. Pérez-Sánchez, and J. Ruiz-Cabello. "Non-destructive seed detection in mandarins: Comparison of automatic threshold methods in FLASH and COMSPIRA MRIs." *Postharvest Biology and Technology*, vol. 47, no. 2, pp. 189-198, 2008.

[3] M. Ruiz-Altisent, L. Ruiz-Garcia, G. P. Moreda, R. Lu, N. Hernandez-Sanchez, E. C. Correa, B. Diezma, B. Nicolai, and J. Garcia-Ramos. "Sensors for product characterization and quality of specialty crops—A review." *Computers and Electronic in Agriculture*, vol. 74, no. 2 pp. 176-194, 2010.

[4] O. Kleynen, V. Leemans, and M-F. Destain. "Development of a multi-spectral vision system for the detection of defects on apples." *Journal of Food Engineering*, vol. 69, no.1, pp. 41-49, 2005.

[5] Y. Yacob, H. Ahmad, P. Saad, R. Aliana, A. Raof, and S. Ismail. "A comparison between X-ray and MRI in postharvest non-destructive detection method." In *Proceedings of the International Conference on Information Technology and Multimedia at UNITEN (ICIMU'05), Malaysia*. 2005.

[6] B. Zion, M. J. McCarthy, and P. Chen. "Real-time detection of pits in processed cherries by magnetic resonance projections." *LWT-Food Science and Technology*, vol. 27, no. 5, pp. 457-462, 1994.

[7] W.L. Kerr, C. J. Clark, M. J. McCarthy, and J. S. De Ropp. "Freezing effects in fruit tissue of kiwifruit observed by magnetic resonance imaging." *Scientia horticulturae*, vol. 69, no. 3, pp. 169-179, 1997.

[8] L. Zhang and M.J. McCarthy, "Measurement and evaluation of tomato maturity using magnetic resonance imaging" *Postharvest Biology and Technology*, vol. 67, pp. 37-43, 2012.

[9] R. G. Gamble, "Non-Invasive Determination of Freezing Effects in Blueberry Fruit Tissue by Magnetic Resonance Imaging." *Journal of food science*, vol. 59, no. 3 pp. 571-573, 1994.

[10] S. L Duce, T. A. Carpenter, and L. D. Hall, "Nuclear magnetic resonance imaging of fresh and frozen courgettes." *Journal of food engineering* vol.16, no. 3, pp.165-172, 1992.

[11] Y. Geya, T. Kimura, H. Fujisaki, Y. Terada, K. Kose, T. Haishi, and Y. Sekozawa, "Longitudinal NMR parameter measurements of Japanese pear fruit during the growing process using a mobile magnetic resonance imaging system," *Journal of Magnetic Resonance*, vol. 226, pp.45-51, 2013.

[12] R. R. Milczarek, M. E. Saltveit, T. C. Garvey, and M. J. McCarthy. "Assessment of tomato pericarp mechanical damage using multivariate analysis of magnetic resonance images." *Postharvest Biology and Technology*, vol. 52, no. 2, pp. 189-195, 2009.

[13] J. J Gonzalez, R. C Valle, S. Bobroff, W.V Biasi, E. J. Mitcham,

- and M. J. McCarthy, "Detection and monitoring of internal browning development in 'Fuji' apples using MRI," *Postharvest biology and technology*, vol. 22, no.2, pp. 179-188, 2001.
- [14] N. Hernandez-Sanchez, B. P. Hills, N. Marigheto, "An NMR study on internal browning in pears" *Postharvest Biol. Technol.* Vol. 44, pp. 260-270, 2007.
- [15] S. Arivazhagan, R. N. Shebiah, S. S. Nidhyandhan, and L. Ganesan. "Fruit recognition using color and texture features." *Journal of Emerging Trends in Computing and Information Sciences* vol. 1, no. 2, pp. 90-94, 2010.
- [16] Y. M. Yacob, A. R. A. M. Shaiful, Z. Husin, R. S. M. Farook, and A. Aziz, "Harum Manis Mango weevil infestation classification using backpropagation neural network." *In Electronic Design, 2008. (ICED 2008), International Conference on IEEE*, pp. 1-6, December, 2008.
- [17] A.M. Aibinu, M.J.E. Salami, A.A. Shafie, N. Hazali and N. Termidzi "Automatic Fruits Identification system Using Hybrid Technique" *IEEE International Symposium on Electronic Design, Test and Application*, vol. 6, pp. 217-220, 2011.
- [18] B.C. In, K. Inamoto, and M. Doi, "A neural network technique to develop a vase life prediction model of cut roses," *Postharvest Biology and Technology*, vol. 52, no. 3, pp. 273-278, 2009.
- [19] D. G. Nishimura, *Principles of magnetic resonance imaging*. Stanford University, pp. 33-102, 1996.
- [20] R. H. Hashemi, W.G. Bradley, C. J. Lisanti, *MRI The Basics*. Lippincott Williams and Wilkins Second edition, pp. 19-55, 2004.
- [21] A. M. Aibinu, M. J. Salami, A. A. Shafie and A.R. Najeeb, "MRI reconstruction using Discrete Fourier transform: A tutorial" *World Academy of science, Engineering and Technology*, vol. 42, pp. 179-185, 2008.
- [22] A. M. Aibinu, M. I. Iqbal, A. A. Shafie, M. J. E. Salami and M. Nilsson "Vascular intersection detection in retina fundus images using a new hybrid approach", *Computers in Biology and Medicine*, vol. 40, no.1, pp. 81-89, 2010.
- [23] Aspect imaging, *M2 Compact High performance MRI system operator manual*, Canada, revised January 6, 2012.
- [24] R. Fisher, S. Perkins, A. Walker, E. Wolfart, "Intensity Histogram" <http://homepages.inf.ed.ac.uk/rbf/HIPR2/histogram.htm>, 2013.
- [25] Z. P. Liang, and P. C. Lauterbur, "An efficient method for dynamic magnetic resonance imaging", *Medical Imaging, Transactions on, 1 IEEE*, vol. 3, no. 4, pp. 677-686, 1994.
- [26] R. C. Gonzalez, R. E. Woods, and S. L. Eddins. *Digital Image Processing*. Prentice-Hall." Inc. Upper Saddle River, New Jersey 7458, pp. 46-665, 2002.
- [27] L. P. Bhaiya, and V. K. Verma, "Classification of MRI Brain Images Using Neural Network". *network*, vol. 2, no.5, pp. 751-756, 2012.
- [28] R. Hecht-Nielsen, "Theory of the backpropagation neural network.," *International Joint Conference in Neural Networks, on IEEE (1989 IJCNN)*, pp. 593-605, June, 1989.
- [29] L. Amirehsan. "A Neural Network based Method for Brain Abnormality Detection in MR Images Using Gabor Wavelets." *International Journal of Computer Applications* vol. 4, no. pp. 79-15, 2010.
- [30] S. Kumar, *Neural Networks : A classroom Approach*. McGraw Hill, pp. 42-205, 2005.